# In situ measurement of dust devil dynamics: Toward a strategy for Mars

David M. Tratt,[1,2] Michael H. Hecht,[1] David C. Catling,[3] Eric C. Samulon,[4] and Peter H. Smith[5]

Received 20 July 2003; revised 16 August 2003; accepted 20 August 2003; published 11 November 2003.

[1] An intensive 3-day dust devil investigation was conducted near Eloy, Arizona, during June of 2001. The goal was to evaluate strategies for observing dust devils on Mars by studying the physics of terrestrial dust devils. As part of this campaign, an instrumented vehicle outfitted with wind, temperature, and pressure sensors was used to intercept and penetrate numerous dust devils. Defined analysis of meteorological fields was only possible with knowledge of the whole body motion of a dust devil. One such data set analyzed revealed a dust devil structure characterized by a tangential wind proportional to radius, $r$, inside the warm, low-pressure core of a dust devil, and proportional to $r^{-1/2}$ outside the core. We discuss the implications for optimum measurement strategies. *INDEX TERMS:* 3322 Meteorology and Atmospheric Dynamics: Land/atmosphere interactions; 3307 Meteorology and Atmospheric Dynamics: Boundary layer processes; 3394 Meteorology and Atmospheric Dynamics: Instruments and techniques; 5707 Planetology: Fluid Planets: Atmospheres—structure and dynamics; 0350 Atmospheric Composition and Structure: Pressure, density, and temperature; *KEYWORDS:* dust devils, vortex structure, vortex dynamics, Rankine vortex model, in situ measurements

**Citation:** Tratt, D. M., M. H. Hecht, D. C. Catling, E. C. Samulon, and P. H. Smith, In situ measurement of dust devil dynamics: Toward a strategy for Mars, *J. Geophys. Res.*, *108*(E11), 5116, doi:10.1029/2003JE002161, 2003.

## 1. Introduction

[2] Although the occurrence of dust devils on Mars has been recognized since the Viking probes era [*Ryan and Lucich*, 1983; *Thomas and Gierasch*, 1985], it was not until the arrival of the Mars Global Surveyor that their profusion and ubiquity was fully appreciated. The imagery returned by that spacecraft have demonstrated that dust devils on Mars can often be spectacular in scale and dwarf their terrestrial counterparts. They have consequently attracted the attention not only of the scientific community, but also those seeking to ensure the success of landed missions sent to Mars [*National Academy of Sciences*, 2002]. For this reason, the NASA Human Exploration and Development of Space Enterprise selected a package of in situ and remote sensing dust devil measurement instruments to fly on the Mars '03 mission. Called MATADOR (Mars ATmosphere And Dust in the Optical and Radio), this multi-institutional development was led by the University of Arizona's Lunar and Planetary Laboratory. The loss of the Mars '98 probes led inter alia to the subsequent cancellation of Mars '03 as it was then conceived and the MATADOR effort was recast as a terrestrial field experiment to ascertain the optimum combination of measurements and instrumentation that would have the greatest impact on dust devil research at Mars. The resulting pilot study was therefore directed at understanding terrestrial dust devils with the goal of evaluating measurement strategies for the study of dust devils on Mars. The culmination of this effort was an intensive three−day field campaign conducted at approximately 32° 37'N, 111° 34'W near Eloy, Arizona during June of 2001. The field site selected consisted of arid regolith terrain adjacent to irrigated agricultural land; a juxtaposition regarded as particularly conducive to dust devil formation [*Rennó et al.*, 1998].

[3] The experiment comprised both a static "base station" as well as an instrumented mobile platform (truck) that was employed to rendezvous with and penetrate dust devils as they approached the site. The static instrument array comprised electromagnetic field remote sensors and a scanning backscatter lidar, along with in situ meteorological sensors to provide a contextual record of the ambient environmental conditions throughout the experiment. As such, the MATADOR experiment represents the most comprehensive suite of instrumentation ever to be deployed in the study of dust devils. Findings obtained from the electromagnetic sensor and lidar data sets are described elsewhere [*Farrell et al.*, 2003; *Carswell et al.*, 2002], while the

[1]Jet Propulsion Laboratory, Pasadena, California, USA.
[2]On leave at Earth Science Technology Office, NASA Goddard Space Flight Center, Greenbelt, Maryland, USA.
[3]Department of Atmospheric Sciences, University of Washington, Seattle, Washington, USA.
[4]Physics Department, University of California, Berkeley, California, USA.
[5]Lunar and Planetary Laboratory, University of Arizona, Tucson, Arizona, USA.

Copyright 2003 by the American Geophysical Union.
0148-0227/03/2003JE002161

emphasis of this paper is on the results obtained from meteorological data acquired during the vehicular portion of the field measurements.

## 2. Experiment Description

[4] The truck-mounted instruments included ultrasonic anemometers, three temperature sensors distributed along a vertical mast, and two redundant differential pressure sensors. The anemometers were positioned ~3.5 m above ground level (AGL) and configured to measure horizontal and vertical wind components at a 5-Hz update rate with an accuracy of ±4% in speed and ±3° in horizontal azimuth. The instrument itself was a commercial unit (FT Technologies FT702/ASF) that at that time was the basis for a wind sensor development intended for deployment aboard the European Beagle 2 Mars lander [*Ringrose et al.*, 2001].

[5] The temperature sensors were commercial type-E (chromel-constantan) thermocouples the sensing elements of which were positioned at a standoff distance of ~15 cm from the mast in order to minimize the influence of the mast and its attendant aerodynamic properties. The disposition distribution of these three sensors along the mast (between 1.5 m and 3.0 m AGL) was intended to provide a measure of the prevailing lapse rate. In the event, these sensors resolved no significant vertical temperature gradients throughout the field operations. The thermocouple/transmitter combination had an overall risetime of ~0.2 s. However, the thermal inertia of the sensor element itself proved somewhat greater than anticipated, resulting in observed decay time constants of order 1 s. While this prevented fully accurate transcription of the temperature excursions induced by dust devil passage it was nevertheless still possible to discern the general behavior of the temperature from the data stream.

[6] The differential pressure sensor was also a commercial device (Motorola MPXV5004G). Based on piezoresistive stress measurement of a silicon diaphragm, it featured on-chip self-compensation for temperature and a measurement resolution capability of 0.001 mbar over a 39-mbar differential pressure range. This sensor was exposed to ambient pressure on one side by means of a 14.2-m long, 2.5-mm bore flexible plastic hose, while the other side of the device measured dust devil air pressure.

[7] The standard Poiseuille formula for flow through a tube as a function of tube dimensions, mean gas pressure, and viscosity of air indicates that the time constant for this tube in response to a pressure change was ~1 ms. This was more than adequate to resolve the slowly varying pressure due to passage of a dust devil. The length of the tube (14.2 m) meant that no pressure deviation due to the dust devil vortex was sensed by the end of the tube measuring ambient air, since the dust devils encountered were typically only of 1–2 m visible radius with the low-pressure core contained largely within this scale.

[8] Both the temperature and differential pressure update rates were 10 Hz. In addition, the ambient absolute atmospheric pressure was measured with a Druck DPI 740 precision pressure indicator.

[9] Although every effort was taken to halt the truck prior to a dust devil encounter, there were nevertheless some instances where the truck was still in motion during the initial stages of vortex penetration. Corrected wind velocities in the true north reference frame were obtained by compensating for truck motion (using speed and heading information derived from an onboard GPS receiver) and for the whole-body motion of the dust devil. The latter was estimated from the prevailing winds before and after the dust devil passage, by interpolating multiple observations of the same dust devil, and from observer log records. (The erratic motion of the typical dust devil makes such an estimation only approximate; we judged the residual uncertainties incurred in this process to be of order ±0.5 m/s in speed and ±15° in direction.) In those cases where sufficient ancillary information was available the tangential and radial dust devil velocity components were calculated by subtracting the inferred translational motion from the corrected wind velocity.

## 3. Field Measurements

[10] Although many dust devils were penetrated during the MATADOR field campaign, comparatively few informative data sets resulted. In large part this was due to the difficulty of judging the relative positions of truck and dust devil with sufficient precision to ensure that the vortex eye traversed the instruments. As a consequence, in many cases the dust devil encounter occurred at the periphery of the vortex. We have selected for discussion here several of the more instructive measurement sets acquired during dust devil encounters made with the instrumented vehicle on June 6 and 7, 2001. All times given are Local Solar Time (LST); for the time and location of these field measurements: LST = UTC − 7h25m. The rapid oscillatory behavior of the differential pressure trace apparent in the early part of each encounter record is a result of the effect of truck motor vibrations acting on the piezoresistive element before its being turned off immediately prior to arrival of the dust devil. Since truck motion impacts the overall data quality, the point at which the truck was stopped is denoted by the vertical broken line in Figures 1–5.

[11] On June 6 multiple encounters with a single dust devil were accomplished in rapid succession. The first encounter (Figure 1, acquired at 12:52:20 LST) was near the periphery of the vortex, so that the observed velocity signature is relatively weak (here $v_h$ is the measured horizontal wind speed). This data set is notable mainly for the sharp nature of the ~1.5-K temperature rise at the closest approach to the eye. In all other cases analyzed the central temperature rise occurred over a significantly longer duration. (The absence of vertical flow data in this and the following two figures is due to the unavailability of that channel on June 6.)

[12] In the next case (Figure 2, acquired on June 6 at 12:53:50 LST) the truck was driven through the same dust devil (signified by the first change of direction in the figure), then stopped in its path. The second change in wind direction thus corresponds to the dust devil passage over the stationary truck. The first (moving) penetration transected the dust devil along a chord somewhat offset from the eye, hence the small observed decrease in wind speed and corresponding slow direction reversal. The second passage appears to be directly through the eye of the dust devil, as indicated by the rapid 180° direction change

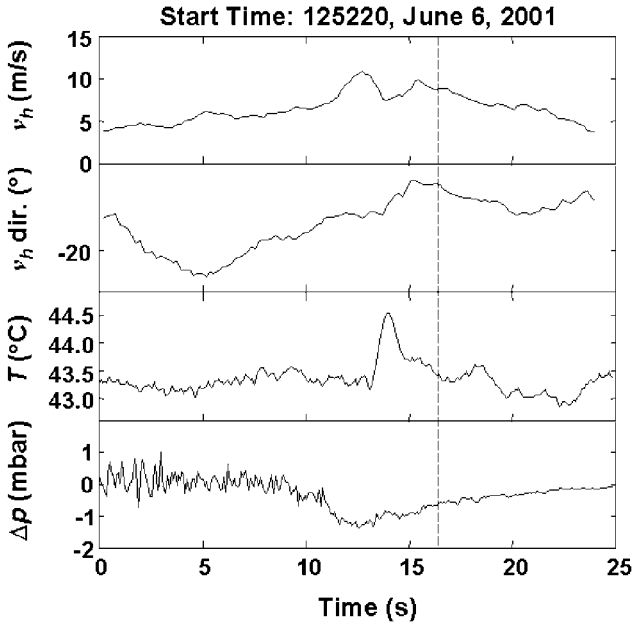


**Figure 1.** Dust devil encounter data acquired at 12:52:20 LST on June 6, 2001. The panels, from top to bottom, are horizontal wind speed, horizontal wind direction, temperature, and pressure relative to the undisturbed ambient air pressure. The vertical broken line signifies the time at which the truck is stopped.

and the corresponding drop to near zero velocity. During traversal of the vortex a 3-K rise in temperature and 1-mbar pressure drop were recorded.

[13] Figure 3 was acquired on June 6 at 12:54:30 LST during a third encounter with the same dust devil represented in the previous two figures, using a repeat of the procedure described above for Figure 2. All indicators suggest that these measurements were made close to, though not coincident with, the vortex eye.

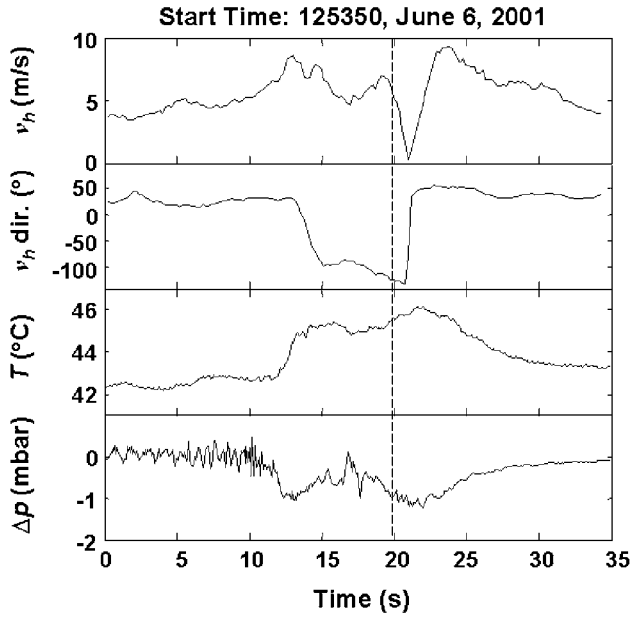


**Figure 2.** Dust devil encounter data acquired at 12:53:50 LST on June 6, 2001; same dust devil as represented in Figure 1.

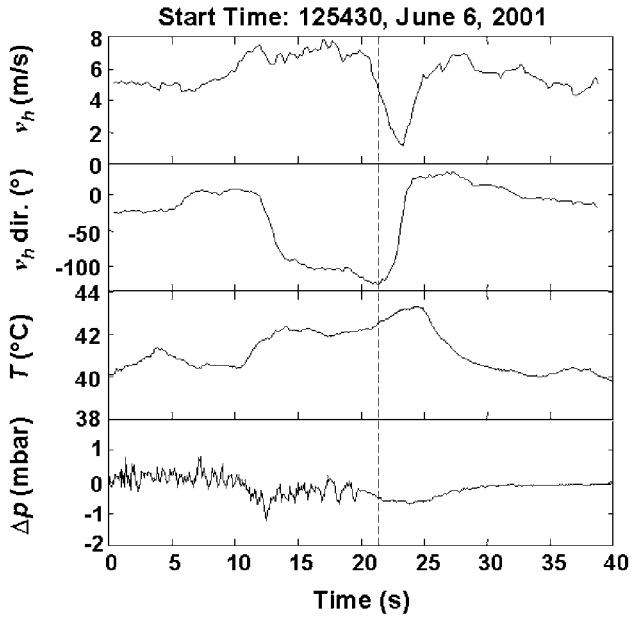


**Figure 3.** Dust devil encounter data acquired at 12:54:30 LST on June 6, 2001; same dust devil as represented in Figures 1 and 2.

[14] The data shown in Figure 4 were acquired on June 7 at 13:40:50 LST. On this date the vertical wind sensing

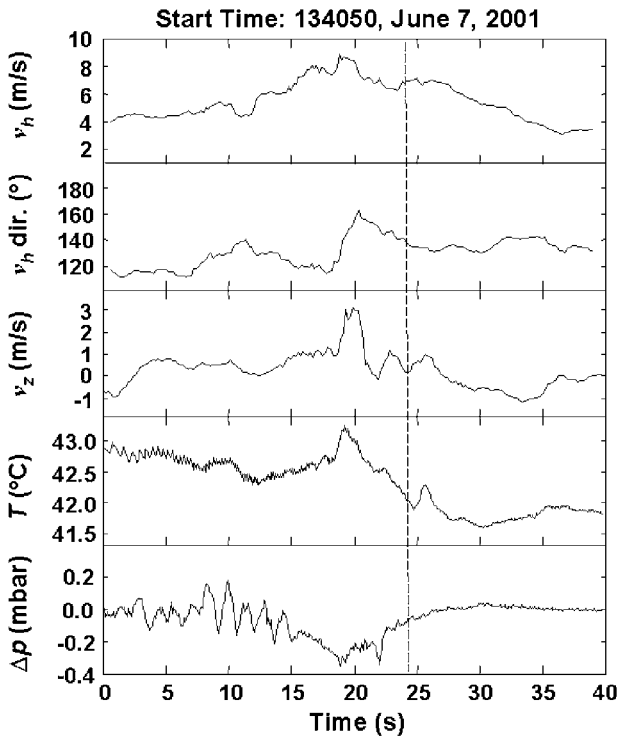


**Figure 4.** Dust devil encounter data acquired at 13:40:50 LST on June 7, 2001.

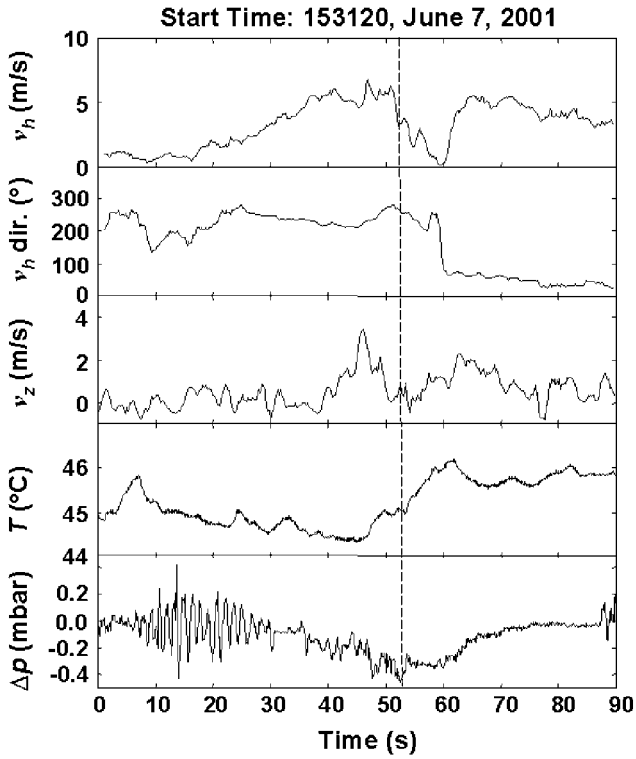


**Figure 5.** Dust devil encounter data acquired at 15:31:20 LST on June 7, 2001.

channel was functional. Although the lack of a central horizontal wind speed decrease and the weak pressure and temperature signatures connote that this encounter did not involve penetration of the eye, the measured vertical updraft at closest approach to the vortex eyewall is nevertheless clearly resolved and 2–3 m/s in magnitude.

[15] The data given in Figure 5, acquired on June 7 at 15:31:20 LST, clearly indicate that the eye of this dust devil exactly traversed the instruments. This is apparent from the observed horizontal wind speed and direction traces, vertical updraft, and pressure signatures. Note that the vertical updraft delineates penetration of the eyewall on either side as the eye transits across the sensor mast. Within the eye itself the vertical flow drops to zero as the stagnation point at the center of the eye is reached [*Rennó et al.*, 1998].

[16] Where a clear record of dust devil dynamics measured diametrically across the vortex is evident, it is possible to reconcile the data with simple thermodynamical theory. The canonical representation of a dust devil can be understood in terms of the whole-body translational motion ($v_{tr}$) with three additional components of wind velocity in the moving reference frame: Tangential ($v_t$), radial ($v_r$), and vertical ($v_z$). The horizontal wind velocity $v_h$ given in Figures 1–5 is the vector sum of $v_t$ and $v_r$. The translational motion is approximately equal to the prevailing wind. As with other cyclonic atmospheric phenomena, the wind field characteristics of a dust devil conform to the Rankine combined vortex model [*Sinclair*, 1973], which specifies that $v_t \propto r$ within the vortex core ($r$ being the radial distance from the vortex center), and $v_t \propto r^{-1}$ outside the core. (The core of a vortex is defined as the zone circumscribed by the radius of maximum tangential wind speed.) The tangential and radial components of velocity are found by correcting for the whole-body motion of the dust devil.

[17] The quality of the encounter data depicted in Figure 2 permits us to assess how well this particular event conformed to the Rankine model. Figure 6 reprises the velocity data from Figure 2 with curve fit overlays added which correspond to the Rankine intracore and extracore regimes. Within the vortex core the tangential velocity component is seen to closely adhere to the proportionality $v_t \propto r$. However, outside the core we observe $v_t \propto r^{-1/2}$, rather than the prescribed $v_t \propto r^{-1}$ (which is also shown for comparison purposes). While its frequency of occurrence with respect to the much smaller scale vortex behavior of dust devils has not been discussed in the literature, this dependence is nevertheless frequently found to describe the tangential wind profile in the extracore regime of hurricanes and tropical storms [*Riehl*, 1963]. *Montgomery and Lu* [1997] have pointed out that this behavior is necessary for the hurricane vortex to maintain quasi-steady state when under the influence of quadratic surface drag (because frictional torques inhibit angular momentum conservation for air parcels moving in proximity to the surface). Similarly, *Rennó and Bluestein* [2001] have considered the effect of angular momentum conservation within the vortex and showed that for angular momentum to be conserved the velocity dependence outside the vortex core must obey $v_t \propto r^{-1}$. (Recent ab initio numerical simulation work independently corroborates this phenomenology and verifies the applicability of the Rankine vortex model above the surface layer [*Toigo et al.*, 2003].) We therefore conclude that the departure from nominal Rankine vortex behavior reported here is a consequence of surface friction effects and that these conditions persisted to an altitude of at least 3.5 m AGL (i.e., the height of the wind sensor).

[18] *Rennó et al.* [2000] provide the following expression linking the maximum tangential velocity $\hat{v}_t$ to the pressure drop $\Delta p$ across the vortex by assuming cyclostrophic

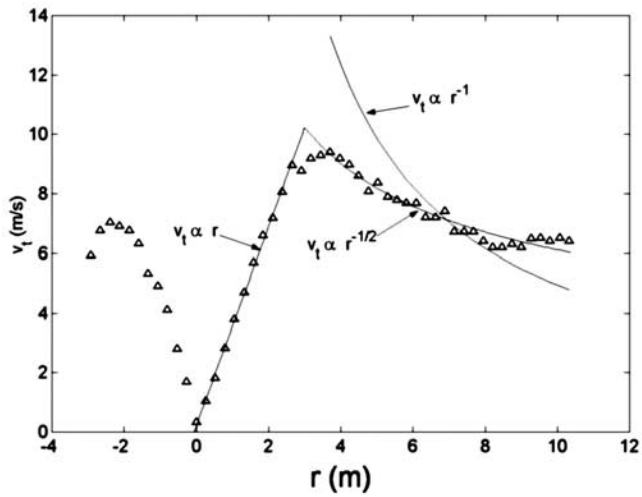


**Figure 6.** Comparison of Figure 2 encounter data (triangles) to the Rankine combined vortex model. The edge of the vortex core is estimated to be ~3.5 m from its center.

**Table 1.** Comparison of Theoretically Derived and Experimentally Measured Maximum Tangential Wind Speed for Two Dust Devil Eye Penetrations

| | | | | $\hat{v}_t$, m/s | |
|---|---|---|---|---|---|
| Data Source | $p$, mbar | $\Delta p$, mbar | $T$, K | Predicted | Measured |
| Figure 2 | 950.0 ± 0.1 | 1.0 ± 0.1 | 316 ± 1 | 9.8 ± 0.5 | 9.4 ± 0.4 |
| Figure 5 | 950.0 ± 0.1 | 0.3 ± 0.1 | 318 ± 1 | 5.4 ± 0.9 | 5.6 ± 0.2 |

balance, i.e., by equating the pressure gradient acceleration to centripetal acceleration:

$$\hat{v}_t \approx \left[\frac{RT\Delta p}{Mp}\right]^{1/2}, \tag{1}$$

where $R$ = 8.314 J K$^{-1}$ mol$^{-1}$, $M$ = 0.029 kg mol$^{-1}$ (the molar mass of air), $T$ and $p$ are the ambient temperature and pressure, respectively, and $\Delta p$ is the pressure drop inside the dust devil relative to ambient. For the case studies depicted in Figures 2 and 5, where the eye was definitively penetrated, we may apply equation (1) to estimate the expected maximum tangential velocity and compare this to the actual measured quantity. The results of this comparison are summarized in Table 1 and show agreement between theory and nature, within experimental uncertainty.

## 4. Discussion

[19] During ex post facto analysis of the many dust devil encounters recorded over the course of the field campaign it was found that full interpretation of the observations was heavily dependent on contextual information derived from visual observer records. To better illustrate why this was the case, we undertook a notional dust devil simulation treatment based on the modified Rankine vortex model referred to above.

[20] Figure 7 indicates the effect of an incomplete knowledge of the perceived dust devil translational velocity and shows the calculated wind vector observations for an idealized dust devil whose centroid passes directly over the sensor. The curves shown are implicitly corrected for the assumed translational whole-body motion (in the direction $y$), but not for the additional, or latent, velocity component $v_x$. The curves in each panel represent progressively larger values of $v_x$, starting from 0 m/s (solid line) and grading in 2-m/s increments to a maximum of 10 m/s (dotted line). We note that neglect of the latent velocity component can make it seem as though the eye of the dust devil did not intersect the sensor, contrary to actuality. These curves should be compared to those of Figure 8, which show the observed wind parameters for a dust devil passing over a sensor with varying degrees of centroid offset. In this figure the solid curve represents a traverse through the center of the eye while the others pass increasingly farther from the eye, with the topmost scan passing through the nominal vortex edge (dotted curve). (Experimental counterparts to many of the modeled transit curves represented in Figures 7 and 8 can be discerned on inspection of Figures 1–5, providing confidence in the essential fidelity of the model employed. A similar procedure has been proposed as a means for identifying dust devil signatures in data returned from the surface of Mars [*Ringrose and Zarnecki*, 2002].)

[21] Comparison of the two scenarios modeled above reveals that, in the absence of compensation for the lateral whole-body motion, the effect of an off-center transit is almost indistinguishable from a center transit with translation. These findings demonstrate why the ability to measure and account for the translational motion of the dust devil is essential, even in the case where the sensor itself is stationary. The implication from this exercise is that unambiguous characterization of dust devil dynamics requires either an array of distributed wind sensors, or an independent measure of the whole-body motion such as a scanning lidar or radar.

## 5. Conclusions

[22] We have described in situ measurements of dust devil dynamics obtained during numerous vortex penetra-

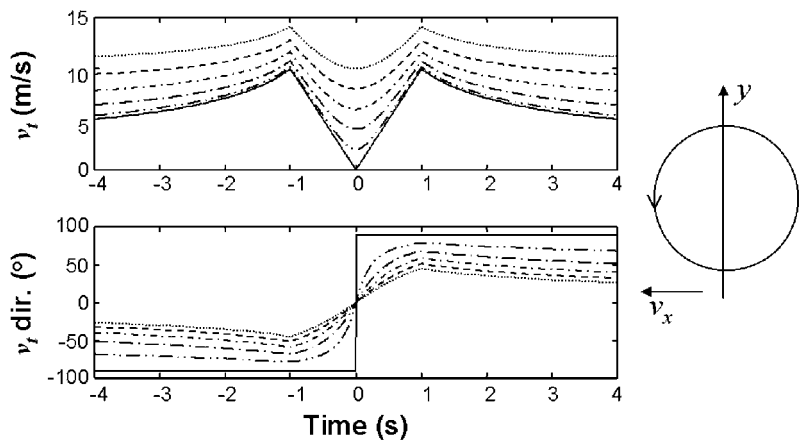


**Figure 7.** Computed wind vector parameters for a dust devil (with translational motion along $y$) passing directly over the sensor. Successive curves show the effect of an increasing latent, uncompensated velocity component $v_x$, starting from 0 m/s (solid line) and grading in 2-m/s increments to a maximum of 10 m/s (dotted line).

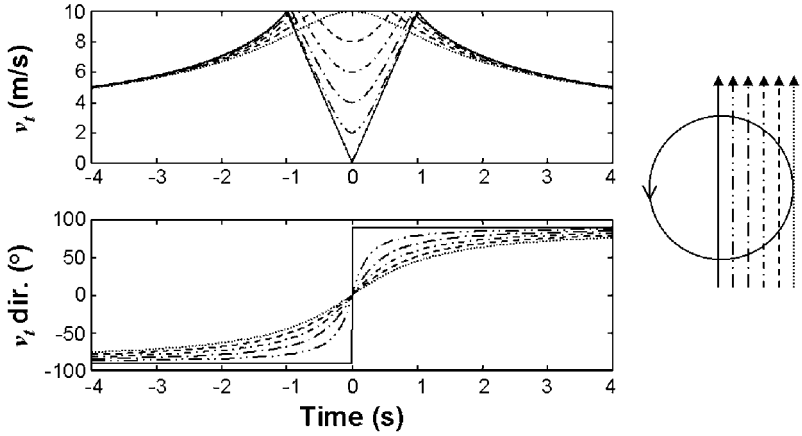


**Figure 8.** Computed wind vector parameters for a dust devil passing over a sensor. The solid curve represents a traverse through the center of the eye while the others pass increasingly farther from the eye. The topmost scan (dotted line) passes through the nominal vortex edge.

tions with a vehicle mounted instrument suite. Elevated temperature, pressure drop, and vertical flow during traversal of the vortex eye were clearly resolved in several of the encounters. In addition, the modeled wind signature has been shown to be open to ambiguous interpretation, depending on the precise nature of the encounter. In particular, the difficulty entailed in distinguishing passage through a dust devil with lateral velocity from passage off-center through a larger dust devil implies that a fully comprehensive depiction of dust devil dynamics requires either a distributed array of in situ wind sensors, or an independent measure of the whole-body motion such as can be provided by a scanning lidar or radar system.

[23] There are reports in the recent literature describing full-body dust devil structure measurements with X-band [*Wurman et al.*, 1997] and W-band [*Bluestein and Pazmany*, 2000] Doppler radars. However, although the use of lidar to study dust devils was not unprecedented prior to the MATADOR campaign [*Schwiesow and Cupp*, 1976; *Jeffreys et al.*, 1976; *Schwiesow et al.*, 1977], there are no apparent published reports of similar investigations in the last 25 years. Furthermore, these early studies were somewhat exploratory in scope and extent. The current availability of more flexible and effective scanning and closed-loop tracking technology for lidar systems should make for more tractable dust devil studies in the present era by removing some of the element of serendipity to which earlier studies were subject. The outcome of this study verifies the original MATADOR concept in that the most effective approach to the comprehensive characterization of dust devils in the field is inferred to be a combination of in situ and remote sensing instruments.

[24] **Acknowledgments.** This work was carried out by the Jet Propulsion Laboratory, California Institute of Technology, under contract with the National Aeronautics and Space Administration. Planning and site selection for the field operations were undertaken by Nilton Rennó. The authors are especially grateful to Greg Delory for his indispensable assistance in integrating the instrumentation and data system for the field operations.

## References

Bluestein, H. B., and A. L. Pazmany, Observations of tornadoes and other convective phenomena with a mobile, 3-mm wavelength, Doppler radar: The spring 1999 field experiment, *Bull. Am. Meteorol. Soc.*, *81*, 2939–2951, 2000.

Carswell, A. I., V. I. Podoba, A. Ulitsky, D. V. Michelangeli, D. Lyons, P. A. Taylor, and W. Weng, Lidar dust devil measurements for future Mars atmospheric studies, in *Lidar Remote Sensing in Atmospheric and Earth Sciences: 21st International Laser Radar Conference*, edited by L. R. Bissonnette, G. Roy, and G. Vallee, pp. 767–769, Def. Res. and Dev. Can., Québec, Canada, 2002.

Farrell, W. M., et al., Electric and magnetic signatures of dust devils from the 2000–2001 MATADOR desert tests, *J. Geophys. Res.*, *108*, doi:10.1029/2003JE002088, in press, 2003.

Jeffreys, H. B., J. W. Bilbro, C. Dimarzio, C. Sonnenschein, and D. Toomey, The remote measurement of tornado-like flows employing a scanning laser Doppler system, in *Preprint Volume: 17th Conference on Radar Meteorology*, pp. 307–312, Am. Meteorol. Soc., Boston, Mass., 1976.

Montgomery, M. T., and C. Lu, Free waves on barotropic vortices. Part I: Eigenmode structure, *J. Atmos. Sci.*, *54*, 1868–1885, 1997.

National Academy of Sciences, *Safe on Mars: Precursor Measurements Necessary to Support Human Operations on the Martian Surface*, 64 pp., Natl. Acad. Press, Washington, D. C., 2002.

Rennó, N. O., and H. B. Bluestein, A simple theory for waterspouts, *J. Atmos. Sci.*, *58*, 927–932, 2001.

Rennó, N. O., M. L. Burkett, and M. P. Larkin, A simple thermodynamic theory of dust devils, *J. Atmos. Sci.*, *55*, 3244–3252, 1998.

Rennó, N. O., A. A. Nash, J. Lunine, and J. Murphy, Martian and terrestrial dust devils: Test of a scaling theory using Pathfinder data, *J. Geophys. Res.*, *105*, 1859–1865, 2000.

Riehl, H., Some relations between wind and thermal structure of steady state hurricanes, *J. Atmos. Sci.*, *20*, 276–287, 1963.

Ringrose, T. J., and J. C. Zarnecki, Martian and terrestrial dust devils, *Proc. Lunar Planet. Sci. Conf. 33rd*, abstract 1183, 2002.

Ringrose, T. J., J. C. Zarnecki, M. C. Towner, S. Kapartis, and R. Strachan, Martian dust devil detection with the Beagle 2 wind sensor, *Proc. Lunar Planet. Sci. Conf. 32nd*, abstract 1281, 2001.

Ryan, J. A., and R. D. Lucich, Possible dust devils, vortices on Mars, *J. Geophys. Res.*, *88*, 11,005–11,011, 1983.

Schwiesow, R. L., and R. E. Cupp, Remote Doppler velocity measurements of atmospheric dust devil vortices, *Appl. Opt.*, *15*, 1–2, 1976.

Schwiesow, R. L., R. E. Cupp, M. J. Post, R. F. Abbey Jr., and P. C. Sinclair, Velocity structures of waterspouts and dust devils as revealed by Doppler lidar measurements, in *Preprint Volume: 10th Conference on Severe Local Storms*, pp. 116–119, Am. Meteorol. Soc., Boston, Mass., 1977.

Sinclair, P. C., The lower structure of dust devils, *J. Atmos. Sci.*, *30*, 1599–1619, 1973.

Thomas, P., and P. J. Gierasch, Dust devils on Mars, *Science*, *230*, 175–177, 1985.

Toigo, A. D., M. I. Richardson, S. P. Ewald, and P. J. Gierasch, Numerical simulation of Martian dust devils, *J. Geophys. Res.*, *108*(E6), 5047, doi:10.1029/2002JE002002, 2003.

Wurman, J., J. Straka, E. Rasmussen, M. Randall, and A. Zahrai, Design and deployment of a portable, pencil-beam, pulsed, 3-cm Doppler radar, *J. Atmos. Oceanic Technol.*, *14*, 1502–1512, 1997.

D. C. Catling, Department of Atmospheric Sciences, University of Washington, Seattle, WA 98195, USA.

M. H. Hecht, Jet Propulsion Laboratory, 4800 Oak Grove Drive, Pasadena, CA 91109, USA.

E. C. Samulon, Physics Department, University of California, Berkeley, CA 94720, USA.

P. H. Smith, Lunar and Planetary Laboratory, University of Arizona, Tucson, AZ 85721, USA.

D. M. Tratt, Earth Science Technology Office, NASA Goddard Space Flight Center, Code 407, Greenbelt, MD 20771, USA. (dtratt@esto.nasa.gov)